CPQ Medicine (2018) 2:2
Research Article

Optimal Scheduling of Combination of Photodynamic Therapy with Anti-Angiogenic Therapy for Effective Control of Local Tumor and Distant Metastasis

Arshi Malik[1*], Mohamed Abd Ellatif [1,4], Basiouny El-Gamal[1], Mohammed Amanullah[1], Sarah Afaq[1], Sayed Saleem Haider[1], Awad Saeed Al-Samghan[2] & Mohammed Yahia Alasmary[3]

[1]*Department of Clinical Biochemistry, College of Medicine, King Khalid University, Abha, Saudi Arabia*

[2]*Department of Family and Community Medicine, College of Medicine, King Khalid University, Abha, Saudi Arabia*

[3]*Department of Internal Medicine, Najran University, Najran, Saudi Arabia*

[4]*Department of Medical Biochemistry, Faculty of Medicine, Mansoura University, Mansoura, Egypt*

[*]**Correspondence to:** Dr. Arshi Malik, Department of Clinical Biochemistry, College of Medicine, King Khalid University, Abha, Saudi Arabia.

Copyright

Received: 03 July 2018

Published: 03 August 2018

Keywords: *Metastasis; Angiogenesis; Avastin; Photodynamic Therapy*

Abstract

Angiogenesis is an important component in tumor development, progression and spread. As a result, there are ongoing efforts to combine existing cytotoxic therapy with anti-angiogenic therapy to enhance the efficacy of cancer treatment. However, the optimal scheduling of anti-angiogenic therapy with cytotoxic therapy, although crucial for maximizing treatment efficacy, remains unclear. Here, we investigated an optimal protocol for combining Avastin anti-angiongenic therapy with photodynamic therapy (PDT), a cytotoxic therapy for various diseases

including cancer. We demonstrate that PDT leads to a temporally-transient regulation of vascular endothelial growth factor (VEGF) following treatment. More importantly, combination Avastin therapy was most effective in inhibiting lung metastasis when delivered around the peak of VEGF response following PDT. Considering that temporally transient VEGF regulation was observed following PDT, radiotherapy and chemotherapy, optimal scheduling of combination anti-angiogenic therapy based on temporal dynamics of the VEGF response has implications in a wide range of cancer treatments.

Abbreviations

PDT - Photodynamic Therapy.
VEGF – Vascular Endothelial Growth Factor
BPD - Benzoporphyrin derivative
ELISA - Enzyme Linked Immunosorbent Assay

Introduction

Angiogenesis, or sprouting of new blood vessels, is a critical component in the development of primary, recurrent and metastatic tumor [1]. As a result, strategies to inhibit the angiogenic process have been extensively investigated as an approach to treat local and distant disease. Monotherapies using anti-angiogenic agents so far resulted in modest clinical response, suggesting to the need for combination with cytotoxic therapies for enhanced tumor control and clinical outcome [2]. Combination of anti-angiogenic therapy with cytotoxic therapy has shown positive outcome in various preclinical studies [3-5]. However, these promising results did not always translate to clinical efficacy [6], demonstrating the complexity of combination strategies.

The efficacy of combination strategies can be enhanced by understanding and exploiting the mechanism of interaction between anti-angiogenic therapy and cytotoxic therapy [7,8]. Although such mechanismsare still being elucidated [6], several hypotheses have been proposed. Neo-adjuvant anti-angiogenic therapy could lead tovascular normalization, in which subsequent tumor oxygenation and physiological changes enhance the efficacy of radiotherapy and chemotherapy [9,10]. It is also suggested that radiotherapy and chemotherapy could target endothelial cells, augmenting the anti-vascular effect of anti-angiogenic therapies [11].

Recent reports suggest that various cytotoxic therapies can potentially lead to a pro-angiogenic response. Upregulation of angiogenic cytokines following cytotoxic therapy was observed in preclinical [3,12-14] as well as clinical studies [15-17]. The increased angiogenic response following cytotoxic therapy correlated with poor clinical outcome [17]. Furthermore, suppression of the upregulated angiogenic response resulted in enhanced local tumor control as well as decreased metastasis [3,5]. As a result, inhibition of the pro-angiogenic response following cytotoxic therapy can provide an additional hypothesis for the mechanism of combination anti-angiogenic therapies.

The aim of this study is to investigate VEGF regulation following cytotoxic therapy as a basis for the efficacy of combination anti-angiogenic therapy. Furthermore, we utilized this mechanistic understanding to devise an optimal strategy for scheduling and sequencing combination anti-angiogenic therapy. Complementary to previous studies, we investigated the optimal strategy to effectively control not only the primary tumor but also distant metastasis. In particular, we investigated the effect of the combination treatment strategy on the two major patterns of metastasis: hematogenous as well as lymphatic metastasis [18]. We demonstrate that the temporal dynamics of the VEGF response following cytotoxic therapy provides important insights into the optimal scheduling of combination anti-angiogenic therapy to inhibit lung metastasis.

Materials and Methods

Reagents and cell lines

Avastin anti-VEGF antibody and liposomal benzoporphyrin derivative (BPD) were a kind gift from Genentech (South San Francisco, CA) and QLT (Vancouver, Canada), respectively. PC-3 prostate cancer cells were maintained in F-12K (Mediatech, Herndon, VA) supplemented with 10% fetal calf serum (Invitrogen, Carlsbad, CA), 100 unit's/mL penicillin, 100 Ag/mL streptomycin (Mediatech).

Animal model

Orthotopic prostate tumors were implanted in the prostate of 6-week-old male severe combined immunodeficient mice weighing 20-25 g (Cox Breeding Laboratories, Cambridge, MA). Animals were anesthetized with a 7:1 mixture of ketamine/xylazine. The prostate was exposed by retracting the bladder cranially following laparotomy. $1x10^6$ PC-3 cells in 50% Matrigel (BD Biosciences, San Diego, CA) were injected into the stroma of the prostate ventral lobe. The incision was closed with 2-0 suture. Tumor with a diameter of 4-5 mm was developed at 2 weeks following implantation.

Cancer therapy

For PDT, 0.25 mg/kg liposomal BPD was injected intravenously (i.v.) in the tail vein of the tumored mouse. One hour following photosensitizer delivery, laparotomy was performed to expose the tumor in the prostate. 690 nm diode laser module (High Power Devices, North Brunswick, NJ) was irradiated on the tumor at an irradiance of 100 mW/cm^2 and a fluence of 50 J/cm^2. Following PDT, the incision was closed with 2-0 suture. Avastin was injected intraperitoneally (i.p.) at a dose of 100 ug in 1mL phosphate buffer saline (PBS).

VEGF ELISA

Tumors were harvested at various time points following PDT and frozen in liquid nitrogen. The frozen tumors were pulverized with a tissue homogenizer and lysed in lysis buffer. The total protein concentration was determined using a standard Lowry method. A human VEGF DuoSet enzyme linked immunosorbent assay (ELISA) Development System (R&D Systems, Minneapolis, MN) was used to quantify human VEGF levels. Resulting VEGF concentrations were normalized by total protein concentration.

Assessment of lung metastasis

The number of human AsPC-1 cells metastasized to the lung was quantified from the level of human and mouse GAPDH housekeeping genes. Lung was harvested two weeks following PDT and snap frozen in liquid nitrogen. Frozen lung tissues were pulverized and RNA was extracted using RNeasy Protect Mini Kits (Qiagen, California, USA) according to the manufacturer's instructions. Human GAPDH gene was measured using forward primer, 5'-GAG TCC ACT GGC GTC TTC-3'; reverse primer, 5'-GGA GGC ATT GCT GAT GATC-3'; with a 165-bp amplified fragment (accession number, NM_002046). Mouse GAPDH was used as reference housekeeping gene for controlling the initial amount of cDNA from each sample (accession number, BC0095932; forward primer, 5'-GCC TTC CGT GTT CCT ACC-3'; reverse primer, 5'-GCC TGC TTC ACC ACC TTC-3'; with a 101-bp amplified fragment). Primers were custom synthesized from Invitrogen (Carlsbad, California). Primers were used at 0.5 uM and 95°C for 10 min, followed by amplification of 40 cycles at 60°C for 30 secs, an extension step at 72°C for 20 secs, and denaturation at 95 C for 10 secs. For each specimen, the cycle threshold (Ct)from human GAPDH was normalized by Ct from mouse GAPDH. The normalized Ct was quantified into number of metastatic cells using a standard curve generated with a set of lung lysate from healthy, non-tumored mice mixed with different numbers of AsPC-1 cells (0, 8, 40, 200, 1,000, 5,000, 25,000 and 125,000 cells).

Assessment of lymph node metastasis

Five um thick, paraffin-embedded sections were obtained from iliac lymph node harvested from tumored mice at 2 weeks following PDT. The sections were stained with hematoxylin and eosin (H&E) and investigated under bright field microscopy to identify any metastatic cancer cells.

Western blot

Ex vivo photosensitizer extraction

Prostate tumors were harvested one hour following intravenous injection of 0.25 mg/kg liposomal BPD. The harvested tumors were snap frozen in liquid nitrogen. The frozen tumors were pulverized using a mortar and pestle containing liquid nitrogen. Pulverized tumors were lysed in 25 mL 1% SDS lysis buffer overnight. The tumor lysate was centrifuged at 14,000 rpm for 10 minutes and the supernatant was collected for further analysis. Fluorescence intensity was measured at 680 nm excitation and 690 nm emission. To quantify photosensitizer concentration in the lysis buffer based on the fluorescence intensity, a set of standards were generated by mixing supernatant from lysed prostate tumors with liposomal BPD at a concentration of 0, 0.2, 1.1 and 5.5mg/mL. Lysis buffer photosensitizer concentration was multiplied by the volume of lysis buffer (25 mL) and divided by the tumor weight to estimate the photosensitizer concentration in the tumor.

In vivo fluorescence imaging of photosensitizer delivery

Fluorescence images of the prostate tumor were acquired *in vivo* with an intravital fluorescence microscope described in [19]. Briefly, the microscope is composed of (i) red light emitting diode (LED) illumination (LXHL-LD3C, Lumileds Lighting, San Jose, CA), (ii) 455 nm exciter filter (455/70, Chroma Technology,

Rockingham, VT), (iii) long working distance objective suitable for *in vivo* imaging (M Plan 40x, Mitutoyo, Aurora, IL), (vi) 700 nm emitter filter (HQ700/75, Chroma Technology, Rockingham, VT), and (v) high sensitivity CCD camera (Cascade 512F, Photometrics, Pleasanton, CA). The tumor was imaged one hour following intravenous injection of 0.25 mg/kg liposomal BPD. Exposure time was 200 msec.

Statistical Analysis

Data are presented as the mean ± SE. Significance of the difference in occurrence of metastasis was evaluated using Fisher's exact test for independent binomial proportions. The significance of the difference in all other data was evaluated with unpaired Student's t-test. $P<0.05$ was considered statistically significant.

Results

Post-PDT VEGF response is transient

Tumoral VEGF levels in PDT-treated and non-treated tumors at various time points were quantified *ex vivo* using the ELISA assay. The tumoral VEGF level increased approximately two-fold in PDT-treated mice compared to non-treated mice one day following PDT (Figure 1A). Subsequently, tumoral VEGF level in PDT-treated mice decreased, reaching approximately one-third of non-treated tumors at one week following PDT. The tumoral VEGF level following PDT remained low for up to two weeks. The tumoral VEGF level in non-treated mice remained almost uniform during the two weeks.

Avastin therapy results in decreased tumoral VEGF following PDT

Effect of Avastin therapy, an antibody that blocks VEGF, on tumoral VEGF level was investigated *ex vivo* using the ELISA assay. For two days prior to PDT, 100 ug Avastin was delivered i.p. to the tumored mice. One day following PDT, the VEGF level in tumors treated with both PDT and Avastin was significantly lower than that measured from tumors treated only with PDT ($p<0.05$) and slightly below that from non-treated tumors, although statistically not significant ($p=0.21$) (Figure 1B). Tumoral VEGF level in mice that were treated with both Avastin and PDT remained low at two weeks following PDT.

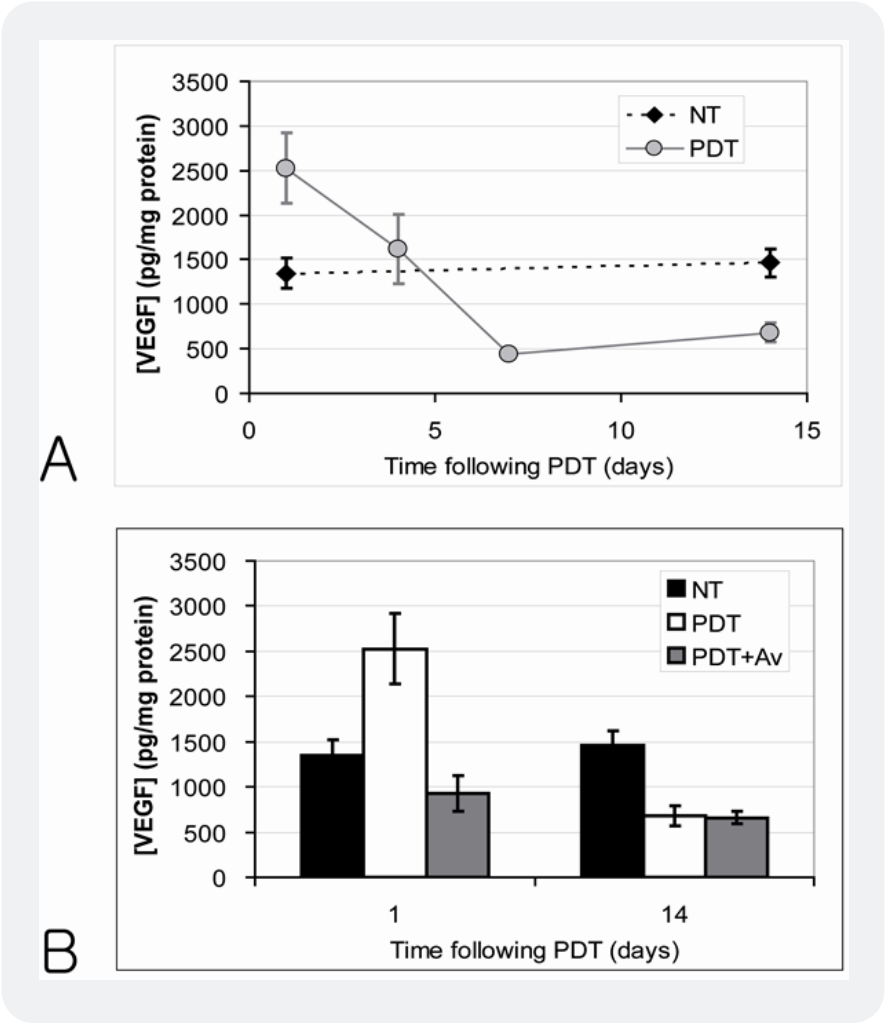

Figure 1: *A. Tumoral VEGF concentration measured from non-treated (solid diamond) and PDT-treated (gray circle) animals at different time points following PDT.*
B. Tumoral VEGF concentration measured from non-treated (slide bars) and PDT-treated (white bars) animals as well as those treated with both PDT and Avastin (gray bars) at one day and 14 days following PDT. VEGF levels were quantified ex vivo using ELISA and normalized by protein content. Error bars show one standard error.

Avastin results in decreased lung metastasis if timed right following PDT

Metastasis of PC-3 human cancer cells to the lungs were evaluated from whole lungs harvested two weeks following PDT. RT-PCR was used to quantify human (cancer cells) RNA levels compared to mouse (host) RNA levels in the lungs. Metastatic burden was characterized using two approaches: (i) by occurrence, which is the percentage of animals with lung metastasis in each group (Figure 2A), and (ii) by the extent, which is the average number of metastasized cancer cells per lung among mice that developed metastasis (Figure 2B). All the non-treated animals developed lung metastasis, with an average of 15,460 cancer cells per lung. Avastin therapy or PDT, when delivered alone, did not result in significant changes in the occurrence or

extent of lung metastasis. Two doses of Avastin, each delivered i.p. at a dose of 100 ug, did not affect the occurrence of lung metastasis. The extent of lung metastasis following Avastin therapy decreased to 6,981 cancer cells/lung, although the difference was not statistically significant (p=0.32). PDT treatment resulted in a non-significant decrease in both occurrence (79%, p=0.22) and extent (2,490 cancer cells/lung, p=0.12) of lung metastasis. Readers may yet ask a question. How can so many people be persuaded to practice self-destruction? The answers bring Freud again into the picture, or rather his nephew, whose name is gradually becoming familiar to many, namely, Edward Bernays and his techniques [7].

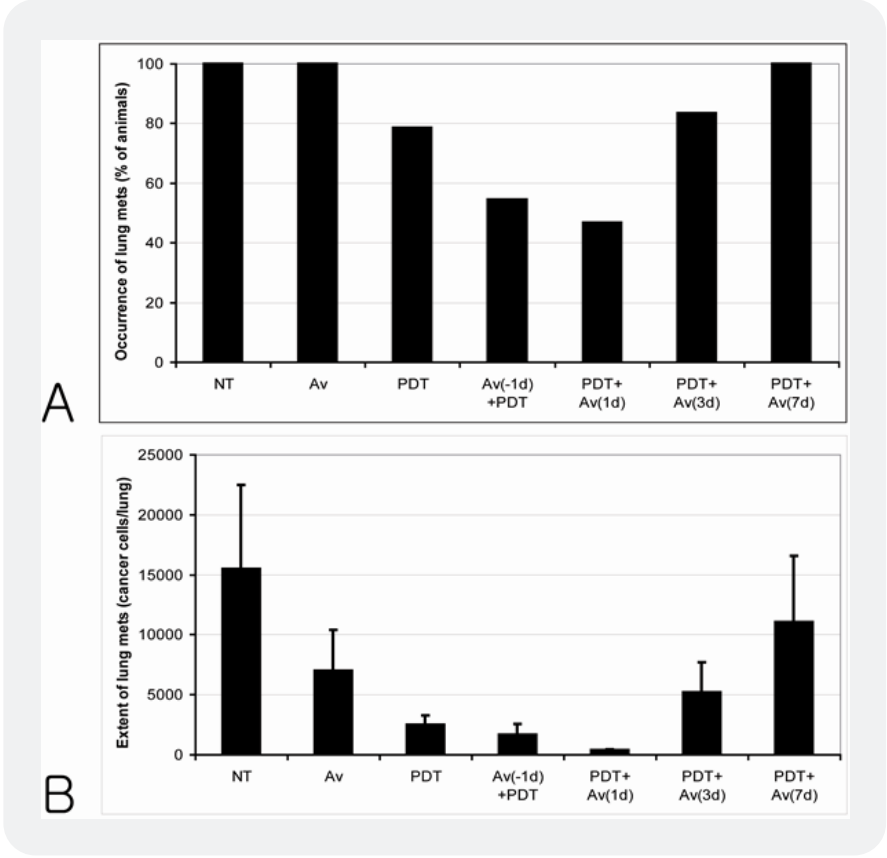

Figure 2: *A. Occurrence of lung metastasis, calculated as the percentage of animals with lung metastasis in each treatment group.*
*B. Extent of lung metastasis, calculated as the average number of cancer cells per lung among animals with lung metastasis in each treatment group. NT: non-treated group (N=14), Av: Avastin monotherapy group (N=12), PDT: PDT monotherapy group (N=16), Av(-1d)+PDT: combination therapy group where Avastin was delivered one day prior to PDT (N=10), PDT+Av(1d): combination therapy group where Avastin was delivered one day after PDT (N=15), PDT+Av(3d): combination therapy group where Avastin was delivered three days after PDT (N=6), PDT+Av(7d): combination therapy group where Avastin was delivered seven days after PDT (N=5). Error bars show on standard error. *: P<0.05 (compared to NT), **: P<0.01 (compared to NT).*

Combination of Avastin and PDT did result in statistically significant decreases in both the occurrence and the extent of lung metastasis only if the Avastin was delivered at an appropriate schedule. When Avastin was delivered immediately after PDT, the occurrence and extent of lung metastasis decreased to 47% ($p<0.05$) and 357 cancer cells/lung ($p<0.05$), respectively. Similarly, the occurrence and extent of lung metastasis decreased to 55% ($p<0.05$) and 1,660 cancer cells/lung ($p=0.09$), respectively, if Avastin was delivered immediately before PDT. However, if Avastin was delivered either 3-days or 7-days following PDT, both the extent and occurrence of lung metastasis was comparable to those of animals treated only with PDT and did not demonstrate any significant change compared to non-treated animals.

PDT and Avastin, either as monotherapy or in combination, does not affect lymph node metastasis

Metastasis of PC-3 human cancer cells to the lymph node was assessed from H&E stained sections. Only the iliac lymph nodes were evaluated in this study as none of the mice developed metastasis to the inguinal lymph node (data not shown). Representative H&E images of normal and metastatic lymph nodes are shown in Figure 3A. Hyperchromatic cancer cells with high nuclear-to-cytoplasmic ratio are observed in the metastatic lymph node but is absent in the normal lymph node. Metastatic burden was determined by the occurrence of metastasis. Unlike lung metastasis, monotherapy nor combination treatment with PDT and Avastin did not have a significant effect on lymph node metastasis. Approximately half of the tumored mice developed lymph node metastasis, regardless of the mode of treatment (Figure 3B). Similar to the role of VEGF-A in vascular angiogenesis, VEGF-C plays an important role in lymphangiogenesis as well as lymphatic metastasis [20]. VEGF-C levels following PDT monotherapy and combination with Avastin were examined with Western blots (Figure 3C). Neither modes of treatment lead to any significant change in tumoral VEGF-C expression.

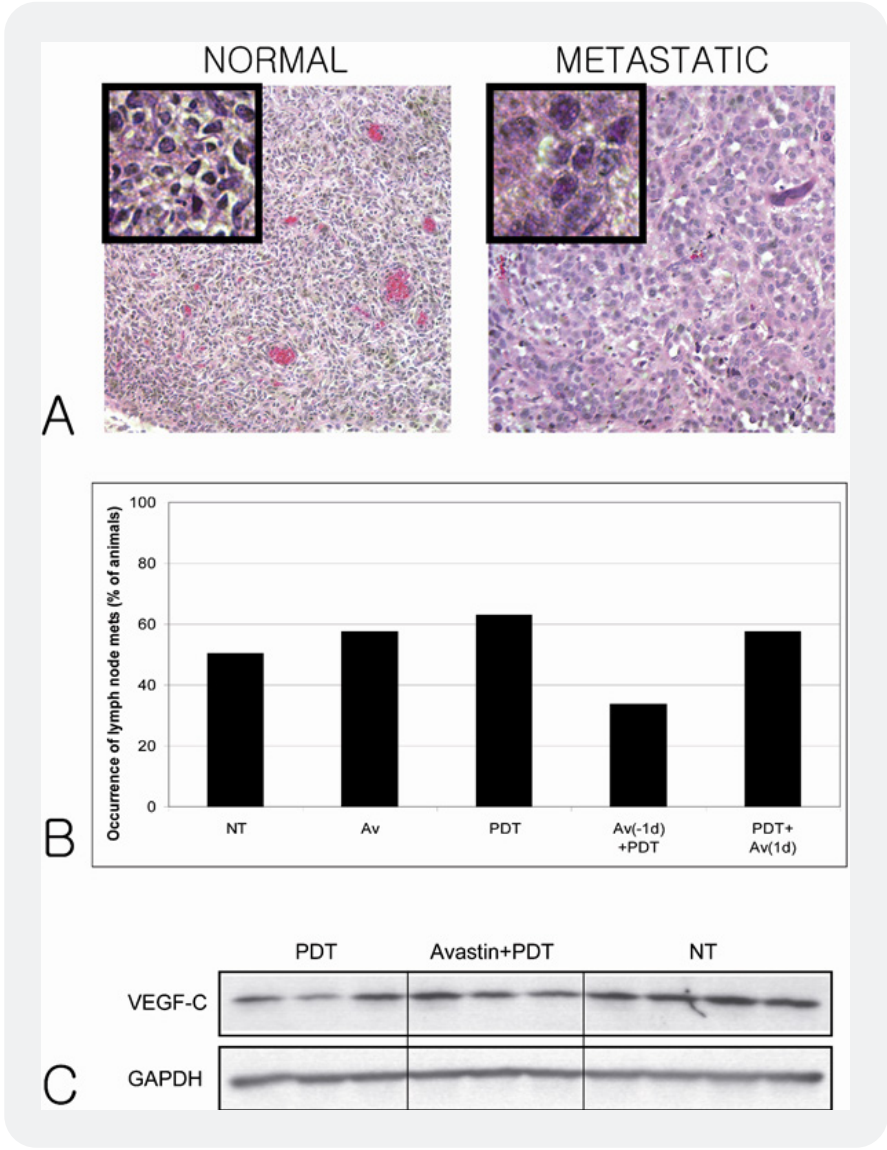

Figure 3: *A. Histological slides from a non-involved (left) and metastatic (right) lymph node imaged using a 10X objective. Inset shows a magnified image with a 40X objective.*
B. Occurrence of lymph node metastasis, calculated as a percentage of animals with lymph node metastasis in each treatment group. NT: non-treated group (N=8), Av: Avastin monotherapy group (N=7), PDT: PDT monotherapy group (N=8), Av(-1d)+PDT: combination therapy group where Avastin was delivered one day prior to PDT (N=6), PDT+Av(1d): combination therapy group where Avastin was delivered one day after PDT (N=7). C. Western blots of VEGF-C and GAPDH in tumors treated with PDT alone (PDT), combination of Avastin and PDT (Avastin+PDT) as well as non-treated tumors (NT).

Additional Avastin therapy does not enhance local tumor control by PDT

The effect of different treatment modalities on local tumor control was assessed by measuring the tumor weight at two weeks following PDT (Figure 4A). The average weight of non-treated tumors was 266 mg. Two doses of 100 ug Avastin did not have a significant effect on primary tumor control. PDT treatment alone resulted in approximately 40 % decrease in tumor weight ($p<0.05$). Combination of Avastin with PDT did not result in additional decrease in primary tumor weight compared to PDT monotherapy. It is interesting to note combination therapy was less effective in local control than PDT alone when Avastin was delivered a day prior to PDT. Decrease in tumor weight was not significant compared to the no treatment group ($p=0.34$).

Avastin delivered prior to PDT affects the delivery of PS

Since blockage of VEGF-A can lead to decreased vascular permeability [21], we investigated whether Avastin therapy prior to PDT had an effect on subsequent intravenous delivery of PS. PS delivery following Avastin therapy was monitored *in vivo* with intravital fluorescence microscopy (Figure 4B). Significant decrease in PS fluorescence was observed in tumors treated with PDT compared to non-treated tumors, suggesting less efficient PS delivery. In order to validate the results of *in vivo* imaging, we harvested the tumors one hour following PS injection and quantified the tumoral PS concentration *ex vivo*. Avastin therapy resulted in a 33 % decrease in tumoral PS concentration compared to non-treated tumors.

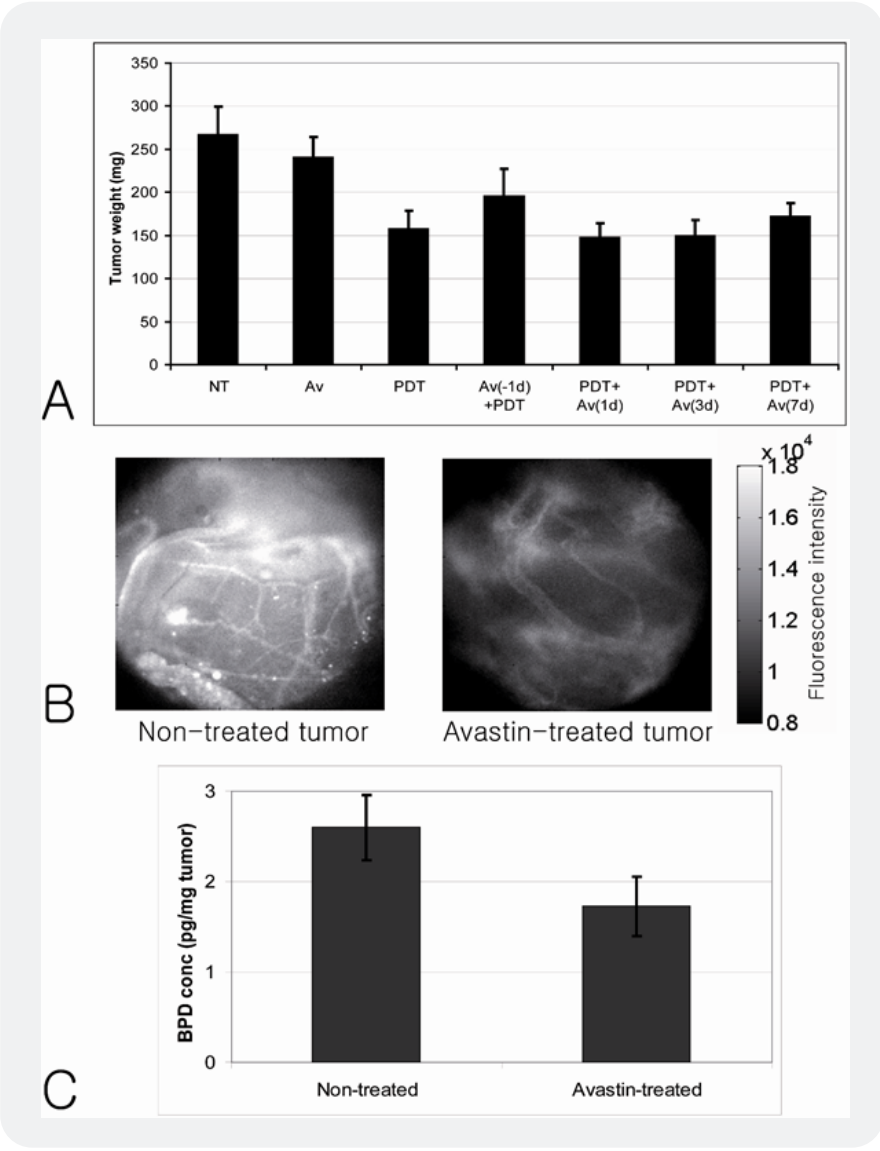

Figure 4: *A. Average tumor weight per animal in each treatment group assessed at two weeks following PDT. NT: non-treated group (N=14), Av: Avastin monotherapy group (N=12), PDT: PDT monotherapy group (N=16), Av(-1d)+PDT: combination therapy group where Avastin was delivered one day prior to PDT (N=10), PDT+Av(1d): combination therapy group where Avastin was delivered one day after PDT (N=15), PDT+Av(3d): combination therapy group where Avastin was delivered three days after PDT (N=6), PDT+Av(7d): combination therapy group where Avastin was delivered seven days after PDT (N=5).*
B. Representative in vivo fluorescence images showing PS distribution in a non-treated tumor (left) as well as Avastin-treated tumor (right) imaged one hour following intravenous injection of PS. C. Average PS concentration quantified ex vivo in non-treated (left) and Avastin-treated (right) tumors one hour following intravenous injection of PS. Error bars show one standard error.: P<0.05 (compared to NT).*

Discussion

A wide range of cytotoxic cancer therapies are effective at controlling the primary tumor. However, their capabilities to control metastasis are less understood. In certain cases, cytotoxic therapies can accelerate metastatic development, as observed in both the clinical and preclinical setting as well as across different treatment modalities [22-27]. Considering that metastasis is the primary cause of cancer-related mortality [28], there is an urgent need to devise treatment strategies to control not only the primary tumor but also metastatic development. The objective of this study was to investigate an optimal treatment regimen that combines PDT, a cytotoxic local therapy, with Avastin, an anti-angiogenic agent, to effectively control metastatic development.

For the treatment of primary tumors, the importance of optimal scheduling in combination therapies has been demonstrated previously. Winkler *et al.* showed that anti-angiogenic treatment using VEGFR2-blocking antibody created a dynamic change in tumor oxygenation [9]. Subsequent radiation therapy was most effective in local tumor control only when it was delivered during the normalization window, or the time of maximal tumor oxygenation. In a separate study, Williams *et al.* found that VEGFR2 tyrosine kinase inhibitor was more effective when it was delivered sequentially following, rather than concurrently with, radiation therapy [29]. These studies reiterate the significance of understanding and exploiting appropriate physiological changes to enhance the efficacy of combination therapies. However, optimal scheduling of combination therapies to control metastatic development is not well understood. This is the first report investigating the optimal scheduling of anti-angiogenic therapy with PDT-based cytotoxic therapy to effectively inhibit metastasis.

We focused on a combination treatment strategy based on anti-angiogenic therapy because our group as well as others observed a pro-angiogenic response including VEGF upregulation following cytotoxic cancer therapy [3,19,30]. Furthermore, inhibition of the pro-angiogenic response was effective in controlling the primary tumor [31-33]and metastasis [26,34]. In this study, we investigated an optimal schedule for the administration of Avastin anti-angiogenic therapy in combination with PDT. In particular, we focused on the significance of the temporally-transient tumoral VEGF response following PDT, in which the peak response occurred one day following PDT. A combination, low-dose Avastin therapy with PDT resulted in a significant 50 % reduction in the occurrence of lung metastasis only when Avastin delivery was scheduled appropriately to target the peak VEGF response following PDT. A same dose of combination anti-angiogenic therapy did not help control lung metastasis when delivered under other scheduling protocols.

The potential mechanism of how the transient increase in VEGF expression following cytotoxic therapy contributes to the development of lung metastasis is complex. Tumoral VEGF expression can lead to various local effects involved in metastasis. VEGF can lead to increased vascular permeability, which can facilitate the intravasation of tumor cells into the tumor vasculature. Furthermore, VEGF can help tumor cells survive at a new target organ by helping recruit new vasculature [1]. VEGF could also stimulate the endothelial cells and pericytes to help develop metastatic micronodules during intravasation [35]. In addition to interaction with tumor vasculature, VEGF can also directly stimulate tumor cells and promote their migration and invasion to facilitate metastasis [36,37]. Regardless of the mechanisms, results of this study point to the significance of the temporal VEGF regulation following cytotoxic cancer therapy as an important regulator of metastasis.

It is particularly important to note that temporally transient VEGF response was observed previously in various studies following PDT, radiotherapy and surgery [38-41]. This suggests that optimal scheduling of combination anti-angiogenic therapy is potentially applicable to a wide range of cytotoxic cancer therapies. The molecular mechanism of temporal regulation of VEGF following cytotoxic therapy is complex. Various molecular mechanisms can induce VEGF overexpression following cytotoxic therapy, including hypoxia, inflammatory response and stress signaling [31,40,42,43]. VEGF expression levels subsequently decrease with time as the growth-factor inducing cancer cells die from cytotoxic therapy or the tumor tissue is re-oxygenated by the pro-angiogenic response [38].

It is interesting to note that the combination Avastin therapy decreased the tumoral VEGF levels comparable to non-treated tumors (Figure 1B). Yet the occurrence of lung metastasis with combination therapy was significantly lower than non-treated animals (Figure 2A). At the same time, suppression of constitutively-expressed tumoral VEGF with Avastin monotherapy did not affect the occurrence of lung metastasis. These results suggest that the acute VEGF expression following PDT plays a particularly important role in the subsequent development of lung metastasis. Recently, Roodkink *et al.* [44] suggested a differential role of constitutively-expressed VEGF as well as hypoxia-induced VEGF. Normoxic tumor regions with homogeneous distribution of constitutively expressed VEGF were characterized by dense blood vessels. On the other hand, tumor regions of hypoxia-induced VEGF expression presented low density of dilated vessels. Similarly, acute VEGF expression following cytotoxic therapy may result in vascular response and metastatic potential different from constitutively-expressed, baseline VEGF expression.

In our study, a relatively low dose of Avastin (100 ug/injection, 2 sequential injections) significantly inhibited metastasis when combined optimally with PDT. Avastin and A4.6.1 (murine antibody equivalent of Avastin), either as monotherapy or in combination, are often administered at multiple days spanning several weeks to achieve an effective a positive outcome [45]. In particular, two-week-long administration of angiostatin anti-angiogenic therapy was required to significantly reduce the metastatic burden when combined with radiotherapy [34]. A short-term anti-angiogenic therapy for two days did not reduce the post-treatment metastatic outcome. The results from our study suggest that optimal scheduling can potentially help reduce the dose of combination anti-angiogenic therapy and yet achieve a significant outcome.

In addition to local effects, acute VEGF regulation following PDT could potentially lead to systemic consequences. Blocking angiogenic molecules in the primary tumor can systemically inhibit angiogenesis at a secondary site and suppress metastatic development [46,47]. Similarly, VEGF upregulation in the primary tumor may also lead to systemic consequences, promoting angiogenesis and metastatic development at the secondary site. To test this hypothesis, we also measured the serum VEGF levels at various time points following PDT. However, we did not detect VEGF levels in the circulation within two weeks following PDT (data not shown), suggesting post-PDT VEGF upregulation is confined in the local tumor and may not have systemic effects in our tumor model.

In contrast to lung metastasis, inhibition of tumoral VEGF response with Avastin did not have an effect on the occurrence of lymph node (Figure 3B). Although the mechanisms of lymphogenous metastasis are still being elucidated, it is believed that VEGF-C, a growth factor which regulates lymph angiogenesis, plays a critical role [48,49]. More recently, there have been reports that overexpression of VEGF-A could also

induce lymph angiogenesis and promote lymph node metastasis [50]. However, it was also found that VEGF-A could stimulate VEGF-C expression, and it is currently not clear whether VEGF-A overexpression mediates lymph node metastasis directly or indirectly through other lymphangiogenic growth factors [50]. In our study, PDT, either as monotherapy or in combination with Avastin, did not affect VEGF-C expression or the occurrence of lymph node metastasis (Figure 3). These results suggest that neither a transient upregulation of VEGF-A nor blockage of VEGF-A with Avastin may have a significant impact on lymph node metastasis. Additional, direct inhibition of lymphangiogenic growth factors may be necessary to control lymphatic metastasis.

In addition to scheduling, the sequence of administering anti-angiogenic therapy and cytotoxic therapy can have an impact on the outcome. When vascular normalization is targeted, anti-angiogenic therapy should be delivered prior to the delivery of cytotoxic therapy [10]. In other cases, an adjuvant protocol of anti-angiogenic therapy following cytotoxic therapy was more effective [29]. In our study, delivering Avastin one day prior to or following PDT did not have a significant effect on the occurrence of lung metastasis (Figure 2A). This suggests that the scheduling of Avastin therapy to target the peak VEGF response following PDT is more important than their sequence for controlling lung metastasis. However, the sequence of the two treatments did affect the control of the primary tumor. The neoadjuvant protocol, where Avastin is administered one day prior to PDT, resulted in a larger tumor burden compared to the adjuvant protocol, where Avastin was delivered following PDT (Figure 4A). One potential cause can be attributed to the physiological changes following Avastin therapy. One of the functions of VEGF is to induce vascular permeability [2], and the blockage of VEGF can lead to decreased vascular permeability [21]. Similarly, both us *in vivo* and *ex vivo* studies demonstrate that tumoral PS accumulation is significantly impeded when the PS is delivered one day after Avastin therapy. These results emphasize the need to carefully consider both the sequence and scheduling of cytotoxic therapy with anti-angiogenic therapy in order to achieve effective local and distant control. In particular, novel drug delivery strategies using innovative technologies can help realize the optimal sequence and scheduling [51].

The results of this study highlight the need for appropriate tools to monitor the temporal dynamics of VEGF response following cytotoxic therapy for optimal scheduling of combination anti-angiogenic therapy. This is particularly important since the temporal kinetics vary between different tumors and treatment modalities. VEGF expressed in mouse squamous cell carcinoma was upregulated at 6-hours and subsided to below base-line levels 48-hours following PDT [38]. In the normal rat brain, VEGF increased one week following PDT and remained elevated for six weeks [39]. Serum VEGF response in patients undergoing lung resection peaked at 12 hours following surgery [40]. Subcutaneous tumors from various cell lines demonstrated differential VEGF response kinetics when treated with radio immunotherapy [41]. Novel *in vivo* imaging strategies to continuously monitor VEGF expression [52] can help implement the findings of this study in various tumors and treatment modalities.

Conclusion

In conclusion, we investigated the optimal strategy to combine PDT, a cytotoxic cancer therapy, with Avastin, an anti-angiogenic agent, for effective control of metastasis. We found that cytotoxic therapy such as PDT can induce a temporally transient VEGF upregulation. Optimal scheduling of Avastin administration

enabled effective control of lung metastasis even at a relatively low dose. When optimally scheduled, the sequence of PDT and Avastin did not have an effect on the control of lung metastasis. However, the sequence of two therapies did have an effect on the local control. It is important to determine the optimal sequence as well as scheduling of two treatments for effective control of the local tumor as well as distant metastasis.

Bibliography

1. Saaristo, A., Karpanen, T. & Alitalo, K. (2000). Mechanisms of angiogenesis and their use in the inhibition of tumor growth and metastasis. *Oncogene, 19*(53), 6122-9.

2. Hicklin, D. J. & Ellis, L. M. (2005). Role of the vascular endothelial growth factor pathway in tumor growth and angiogenesis. *J Clin Oncol., 23*(5), 1011-27.

3. Gorski, D. H., Beckett, M. A., Jaskowiak, N. T., *et al.* (1999). Blockage of the vascular endothelial growth factor stress response increases the antitumor effects of ionizing radiation. *Cancer Res., 59*(14), 3374-8.

4. Fox, W. D., Higgins, B., Maiese, K. M., *et al.* (2002). Antibody to vascular endothelial growth factor slows growth of an androgen-independent xenograft model of prostate cancer. *Clin Cancer Res., 8*(10), 3226-31.

5. Kosharskyy, B., Solban, N., Chang, S. K., Rizvi, I., Chang, Y. & Hasan, T. A. (2006). Mechanism-based combination therapy reduces local tumor growth and metastasis in an orthotopic model of prostate cancer. *Cancer Res., 66*(22), 10953-8.

6. Jain, R. K., Duda, D. G., Clark, J. W. & Loeffler, J. S. (2006). Lessons from phase III clinical trials on anti-VEGF therapy for cancer. *Nat Clin Pract Oncol., 3*(1), 24-40.

7. Horsman, M. R. & Siemann, D. W. (2006). Pathophysiologic effects of vascular-targeting agents and the implications for combination with conventional therapies. *Cancer Res., 66*(24), 11520-39.

8. Senan, S. & Smit, E. F. (2007). Design of clinical trials of radiation combined with antiangiogenic therapy. *Oncologist., 12*(4), 465-77.

9. Winkler, F., Kozin, S. V., Tong, R. T., *et al.* (2004). Kinetics of vascular normalization by VEGFR2 blockade governs brain tumor response to radiation: Role of oxygenation, angiopoietin-1, and matrix metalloproteinases. *Cancer Cell., 6*(6), 553-63.

10. Jain, R. K. (2005). Normalization of tumor vasculature: An emerging concept in antiangiogenic therapy. *Science, 307*(5706), 58-62.

11. Mauceri, H. J., Hanna, N. N., Beckett, M. A., *et al.* (1988). Combined effects of angiostatin and ionizing radiation in antitumour therapy. *Nature, 394*(6690), 287-91.

12. Brieger, J., Kattwinkel, J., Berres, M., Gosepath, J. & Mann, W. J. (2007). Impact of vascular endothelial growth factor release on radiation resistance. *Oncol Rep., 18*(6), 1597-601.

13. Solban, N., Selbo, P. K., Sinha, A. K., Chang, S. K. & Hasan, T. (2006). Mechanistic investigation and implications of PDT-induction of VEGF in prostate cancer. *Cancer Res., 66*, 1-8.

14. Viloria-Petit, A., Crombet, T., Jothy, S., *et al.* (2001). Acquired resistance to the antitumor effect of epidermal growth factor receptor-blocking antibodies *in vivo*: A role for altered tumor angiogenesis. *Cancer Res., 61*(13), 5090-101.

15. Inoue, Y., Ojima, E., Watanabe, H., *et al.* (2007). Does preoperative chemo-radiotherapy enhance the expression of vascular endothelial growth factor in patients with rectal cancer? *Oncol Rep., 18*(2), 369-75.

16. Nozue, M., Isaka, N. & Fukao, K. (2001). Over-expression of vascular endothelial growth factor after preoperative radiation therapy for rectal cancer. *Oncol Rep., 8*(6), 1247-9.

17. Chan, L. W., Moses, M. A., Goley, E, *et al.* (2004). Urinary VEGF and MMP levels as predictive markers of 1-year progression-free survival in cancer patients treated with radiation therapy: A longitudinal study of protein kinetics throughout tumor progression and therapy. *J Clin Oncol., 22*(3), 499-506.

18. Pantel, K. & Brakenhoff, R. H. (2004). Dissecting the metastatic cascade. *Nat Rev Cancer., 4*(6), 448-56.

19. Solban, N., Selbo, P. K., Sinha, A. K., Chang, S. K. & Hasan, T. (2006). Mechanistic investigation and implications of photodynamic therapy induction of vascular endothelial growth factor in prostate cancer. *Cancer Res., 66*(11), 5633-40.

20. Nathanson, S. D. (2003). Insights into the mechanisms of lymph node metastasis. *Cancer, 98*(2), 413-23.

21. Lichtenbeld, H. C., Ferarra, N., Jain, R. K. & Munn, L. L. (1999). Effect of local anti-VEGF antibody treatment on tumor microvessel permeability. *Microvasc Res., 57*(3), 357-62.

22. O'Brien, C. J., Smith, J. W., Soong, S. J., Urist, M. M. & Maddox, W. A. (1986). Neck dissection with and without radiotherapy: Prognostic factors, patterns of recurrence, and survival. *Am J Surg., 152*(4), 456-63.

23. Slotman, G. J., Mohit, T., Raina, S., Swaminathan, A. P., Ohanian, M., *et al.* (1984). The incidence of metastases after multimodal therapy for cancer of the head and neck. *Cancer, 54*, 2009-14.

24. Von Essen, C. F. (1991). Radiation enhancement of metastasis: A review. *Clin Exp Metastasis., 9*(2), 77-104.

25. Camphausen, K., Moses, M. A., Beecken, W. D., Khan, M. K., Folkman, J. & O'Reilly, M. S. (2001). Radiation therapy to a primary tumor accelerates metastatic growth in mice. *Cancer Res., 61*(5), 2207-11.

26. Kosharskyy, B., Solban, N., Chang, S. K., Rizvi, I., Chang, Y. & Hasan, T. (2006). A mechanism-based combination therapy reduces local tumor growth and metastasis in an orthotopic model of prostate cancer. *Cancer Res., 66*(22), 10953-8.

27. Agemy, L., Harmelin, A., Waks, T., *et al.* (2008). Irradiation enhances the metastatic potential of prostatic small cell carcinoma xenografts. *Prostate, 68*, 530-9.

28. Weigelt, B., Peterse, J. L. & van 't Veer, L. J. (2005). Breast cancer metastasis: Markers and models. *Nat Rev Cancer., 5*(8), 591-602.

29. Williams, K. J., Telfer, B. A., Brave, S., *et al.* (2004). ZD6474, a potent inhibitor of vascular endothelial growth factor signaling, combined with radiotherapy: Schedule-dependent enhancement of antitumor activity. *Clin Cancer Res., 10*(24), 8587-93.

30. Chung, Y. L., Jian, J. J., Cheng, S. H., *et al.* (2006). Sublethal irradiation induces vascular endothelial growth factor and promotes growth of hepatoma cells: Implications for radiotherapy of hepatocellular carcinoma. *Clin Cancer Res., 12*(9), 2706-15.

31. Ferrario, A. & Gomer, C. J. (2006). Avastin enhances photodynamic therapy treatment of kaposi's sarcoma in a mouse tumor model. *J Environ PatholToxicol Oncol., 25*(1-2), 251-60.

32. Bhuvaneswari, R., Yuen, G. Y., Chee, S. K. & Olivo, M. (2007). Hypericin-mediated photodynamic therapy in combination with avastin (bevacizumab) improves tumor response by downregulating angiogenic proteins. *PhotochemPhotobiol Sci., 6*(12), 1275-83.

33. Jiang, F., Zhang, X., Kalkanis, S. N., *et al.* (2008). Combination therapy with antiangiogenic treatment and photodynamic therapy for the nude mouse bearing U87 glioblastoma. *Photochem Photobiol., 84*(1), 128-37.

34. Gorski, D. H., Mauceri, H. J., Salloum, R. M., Halpern, A., Seetharam, S. & Weichselbaum, R. R. (2003). Prolonged treatment with angiostatin reduces metastatic burden during radiation therapy. *Cancer Res., 63(*2), 308-11.

35. Kusters, B., Kats, G., Roodink, I., *et al.* (2007). Micronodular transformation as a novel mechanism of VEGF-A-induced metastasis. *Oncogene, 26*(39), 5808-15.

36. Chen, J., De, S., Brainard, J. & Byzova, T. V. (2004). Metastatic properties of prostate cancer cells are controlled by VEGF. *Cell Commun Adhes., 11*(1), 1-11.

37. Wey, J. S., Fan, F., Gray, M. J., *et al.* (2005). Vascular endothelial growth factor receptor-1 promotes migration and invasion in pancreatic carcinoma cell lines. *Cancer, 104*(2), 427-38.

38. Uehara, M., Inokuchi, T., Sano, K. & ZuoLin, W. (2001). Expression of vascular endothelial growth factor in mouse tumours subjected to photodynamic therapy. *Eur J Cancer., 37*(16), 2111-5.

39. Jiang, F., Zhang, Z. G., Katakowski, M., *et al.* (2004). Angiogenesis induced by photodynamic therapy in normal rat brains. *Photochem Photobiol., 79*(6), 494-8.

40. Maniwa, Y., Okada, M., Ishii, N. & Kiyooka, K. (1998). Vascular endothelial growth factor increased by pulmonary surgery accelerates the growth of micrometastases in metastatic lung cancer. *Chest, 114*(6), 1668-75.

41. Taylor, A. P., Osorio, L., Craig, R., *et al.* (2002). Tumor-specific regulation of angiogenic growth factors and their receptors during recovery from cytotoxic therapy. *Clin Cancer Res., 8*(4), 1213-22.

42. Solban, N., Selbo, P. K., Sinha, A. K., Chang, S. K. & Hasan, T. (2006). Mechanistic investigation and implications of photodynamic therapy induction of vascular endothelial growth factor in prostate cancer. *Cancer Res., 66*(11), 5633-40.

43. Gomer, C. J., Ferrario, A., Luna, M., Rucker, N. & Wong, S. (2006). Photodynamic therapy: Combined modality approaches targeting the tumor microenvironment. *Lasers Surg Med., 38*(5), 516-21.

44. Roodink, I., van der Laak, J., Kusters, B., *et al.* (2006). Development of the tumor vascular bed in response to hypoxia-induced VEGF-A differs from that in tumors with constitutive VEGF-A expression. *Int J Cancer., 119*, 2054-62.

45. Gerber, H. P. & Ferrara, N. (2005). Pharmacology and pharmacodynamics of bevacizumab as monotherapy or in combination with cytotoxic therapy in preclinical studies. *Cancer Res., 65*(3), 671-80.

46. Sckell, A., Safabakhsh, N., Dellian, M. & Jain, R. K. (1998). Tumor size-dependent inhibition of angiogenesis at a secondary site: An intravital microscopic study in mice. *Cancer Res., 58*(24), 5866-9.

47. O'Reilly, M. S., Holmgren, L., Shing, Y., *et al.* (1994). Angiostatin: A novel angiogenesis inhibitor that mediates the suppression of metastases by a lewis lung carcinoma. *Cell, 79*(2), 315-28.

48. Hoshida, T., Isaka, N., Hagendoorn, J., *et al.* (2006). Imaging steps of lymphatic metastasis reveals that vascular endothelial growth Factor-C increases metastasis by increasing delivery of cancer cells to lymph nodes: Therapeutic implications. *Cancer Res., 66*(16), 8065-75.

49. Hirakawa, S., Brown, L. F., Kodama, S., Paavonen, K., Alitalo, K. & Detmar, M. (2007). VEGF-C-induced lymphangiogenesis in sentinel lymph nodes promotes tumor metastasis to distant sites. *Blood, 109*(3), 1010-7.

50. Hirakawa, S., Kodama, S., Kunstfeld, R., Kajiya, K., Brown, L. F. & Detmar, M. (2005). VEGF-A induces tumor and sentinel lymph node lymphangiogenesis and promotes lymphatic metastasis. *J Exp Med., 201*(7), 1089-99.

51. Sengupta, S., Eavarone, D., Capila, I., *et al.* (2005). Temporal targeting of tumour cells and neovasculature with a nanoscale delivery system. *Nature, 436*(7050), 568-72.

52. Chang, S. K., Rizvi, I., Solban, N. & Hasan, T. (2008). In vivo optical molecular imaging of vascular endothelial growth factor for monitoring cancer treatment. *Clin Cancer Res., 14*(13), 4146-53.